J Intell Manuf (2019) 30:809–820
https://doi.org/10.1007/s10845-016-1282-2

Evaluation of genetic programming-based models for simulating bead dimensions in wire and arc additive manufacturing

Biranchi Panda[1] · K. Shankhwar[2] · Akhil Garg[3] · M. M. Savalani[4]

Received: 13 March 2016 / Accepted: 16 November 2016 / Published online: 26 November 2016

Abstract Wire and arc additive manufacturing (WAAM) is a novel rapid prototyping process that employs gas tungsten arc welding, controlled by a robot, to build complex 3D parts by successive layer deposition technique. Experimental studies on WAAM are useful for understanding the physics of the process however the quantification and optimization of process parameters is difficult due to complex mechanisms involved in WAAM process. In this present work, the measurement of two bead dimensions (bead height and bead width) based on the three inputs (peak current, wire feed speed, and travel speed) is done using the gas tungsten arc welding machine. Experimental study is followed by proposition of two variants of advanced evolutionary algorithms (gene expression programming and multi-gene genetic programming) in formulation of the functional expressions for the two bead dimensions based on the three inputs. The performance analysis of the two proposed models is conducted based on the four statistical error metrics, hypothesis tests and cross-validation. The relationships extracted between the bead dimensions and the three inputs reveals that the peak current influences both the bead height and bead width simultaneously. The findings reported will have a positive implication on the industry in predictive monitoring of the bead dimensions during the WAAM process.

✉ Akhil Garg
akhil@stu.edu.cn

1 IDMEC, Instituto Superior Técnico, Universidade de Lisboa, Lisboa, Portugal

2 Department of Mechanical Engineering, Kalinga Institute of Industrial Technology, Bhubaneswar, India

3 Department of Mechatronics Engineering, Shantou University, Shantou 515063, China

4 Department of Industrial and Systems Engineering, HongKong Polytechnic University, Kowloon, Hongkong

Keywords Wire and arc additive manufacturing · Bead geometry · Multi-gene genetic programming · Modelling

Introduction

In recent years, additive manufacturing (AM) has become a promising technique to fabricate components made of expensive materials for aerospace and automobile industries. Many metal AM techniques such as selective laser sintering, direct metal deposition, electron beam melting and shape deposition manufacturing have been developed to print complex metal shapes out of computerized 3D model (Gibson et al. 2010; Mahapatra and Panda 2013). Among all, wire and arc additive manufacturing (WAAM) has received much concern for its significant advantages of fabricating high dense large scale near net shape components at a low cost in more environmental friendly way (Wang et al. 2011; Brandl et al. 2012). The technology combines arc welding with wire feeding and is able to benefit designers to achieve freedom of their design. It begins with feeding wire into a travelling electric arc and depositing the molten metal sequentially as per described path in computer-aided design (CAD) model. The melting of wire is done by either using a source of laser or a welding torch which is controlled by a robot in an inert atmosphere (Baufeld et al. 2011). This allows obtaining a final product with low oxygen and nitrogen contamination. Also use of wire as a raw material instead of any powder base material allows higher deposition rate and less contamination effect compare to other metal AM processes.

In this WAAM, a gas tungsten arc welding (GTAW) is employed to deposit molten material layer by layer to produce complex prototypes out of 3D model. Robotic systems are most often used to carry out such deposition tasks while all the movements are controlled by the G-code generated from the CAD data (Panda et al. (2016a, b, c); Wang et al. 2015a). Like other AM process, WAAM involves many process parameters that need to be optimized for producing quality prototypes in lesser build time (Tay et al. 2016; Sharma et al. 2016).

Literature reveals that the process is dominated by some parameters such as welding power supply parameters, wire feed speed (WFS), travel speed (TS), arc length, interpass temperature, wire feed angle, gas flow and it is highly necessary to select optimum value of these parameters in order to the achieve a specific target wall width/height requirement as denoted in original CAD data. Therefore, investigations have been done on the effects of arc voltage, travel speed, wire diameter, and arc current on the quality and bead geometries (Baufeld et al. 2011). Many researchers have experimentally studied the effect of process parameters on geometric size, as reported by Oshima et al. (2005), Ouyang et al. (2002), Kazanas et al. (2012), and Ding et al. (2015) but they all considered only one factor in deciding the bead geometry, and thus, their combined effect were not fully explored. For the first time, Williams developed a mathematical model of effective wall width using response surface methodology (RSM) for depositing Ti–6Al–4V parts. The model was based on three input factors and the outcomes were expected to help in designing an expert WAAM system for effective functioning and higher productivity purposes. RSM is one of the statistical experimental design methods designed for developing the optimum process with efficient screening; however, the regression analysis technique may not perform satisfactory on unseen test data and is based on the statistical assumptions (assumption of the model structure ad correlated residuals). Poor performance of the model on the test data leads to poor generalization ability and results in false information of the process input process conditions (Garg and Tai 2012; Garg et al. 2014; Çiçek et al. 2015). A much better alternative among other evolutionary algorithms such as adaptive neuro-fuzzy inference system (ANFIS), artificial neural network (ANN), support vector machine (SVM) is the genetic programming (GP) which evolves the functional relationships between the process parameters automatically (Sohrabpoor et al. 2016; Garg et al. 2014; Panda et al. 2014; Vijayaraghavan et al. 2015; Panda et al. 2016). Significant progress in literature of GP was made which justifies its ability to model and optimize the complex systems (Nie et al. 2013; Wang et al. 2015a, b). Therefore, the present work will explore the ability of the advanced variants of evolutionary algorithms such as GEP and MGGP in performing the task of formulating the decision support models for bead dimensions of WAAM process. The decision support model can not only extrapolate/predict but also suggests the precise selection of process variables for the improvement of WAAM process. Experimental procedure resulting in the data generation is set as input into the framework of these two variants for the processing and analysis. The procedure involving the experimentation planning and the modelling with respect to the three inputs is shown in Fig. 1. Two variants of GP, i.e., MGGP and GEP is used and their performance is compared for predicting bead dimensions (bead width and height) with respect to peak current, wire feed speed, and travel speed. The complexity term based on the minimum order of the polynomial used in the objective function (Structural risk minimization principle (SRM)) (Rao and Murthy 2016) of both these variants is used to investigate the generalization ability of the proposed models. The 2D and 3D plots are generated to measure the effect of each input and their interaction effects on the bead dimensions. The implications arising from the study is discussed in the end.

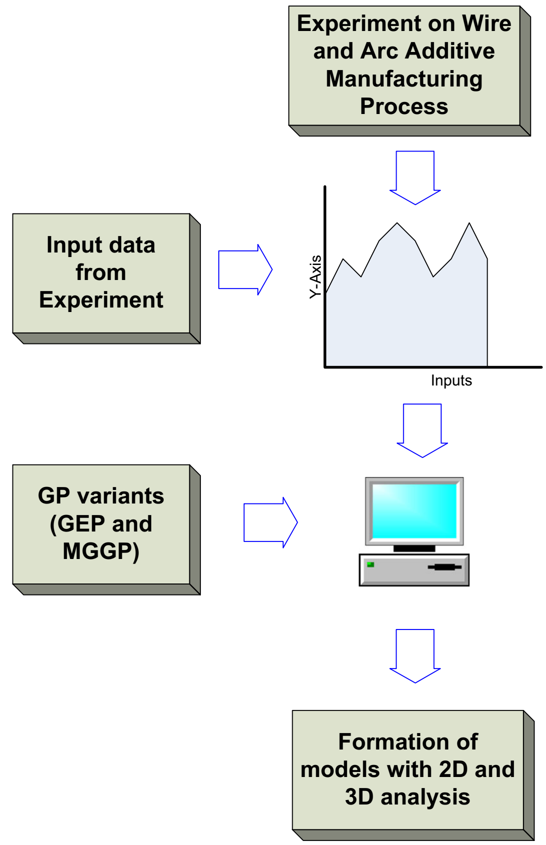

Fig. 1 Complete procedure of experimental and evolutionary algorithms in investigations of bead dimensions of WAAM process

Experimental set-up of WAAM

In this section, the complete set-up of WAAM process is discussed in measurement of bead height (BH) and bead width (BW) based on the peak current, travel speed and wire feed speed. The equipment used in this study and the assumptions behind the experiments are kept same as those discussed in Geng et al. (2015). A GTAW welding machine (EWM, Tetrix 521 Synergic AC/DC) was used as a source of weld power. Other parameters such as the background current, pulse fre-

Table 1 Experimental data obtained from the WAAM process

Peak current (in amp)	Travel speed (m/min)	Wire feed speed (m/min)	BH (in mm)	BW (in mm)
140	4	0.2	1.32	6.26
180	4	0.2	0.95	8.56
140	7	0.2	2.16	6.49
180	7	0.2	1.61	8.59
140	4	0.3	1.02	5.4
180	4	0.3	0.77	7.04
140	7	0.3	1.62	5.53
180	7	0.3	1.24	7.4
126.4	5.5	0.25	1.66	5.24
193.6	5.5	0.25	1.05	8.74
160	2.98	0.25	0.76	6.66
160	8.02	0.25	1.89	6.76
–	–	–		–
–	–	–		–
–	–	–		–
–	–	–		–
160	5.5	0.17	1.65	7.89
160	5.5	0.33	1.07	5.96
160	5.5	0.25	1.27	6.81
160	5.5	0.25	1.31	6.85
160	5.5	0.25	1.27	6.91
160	5.5	0.25	1.25	6.8
160	5.5	0.25	1.29	6.91
160	5.5	0.25	1.26	6.89

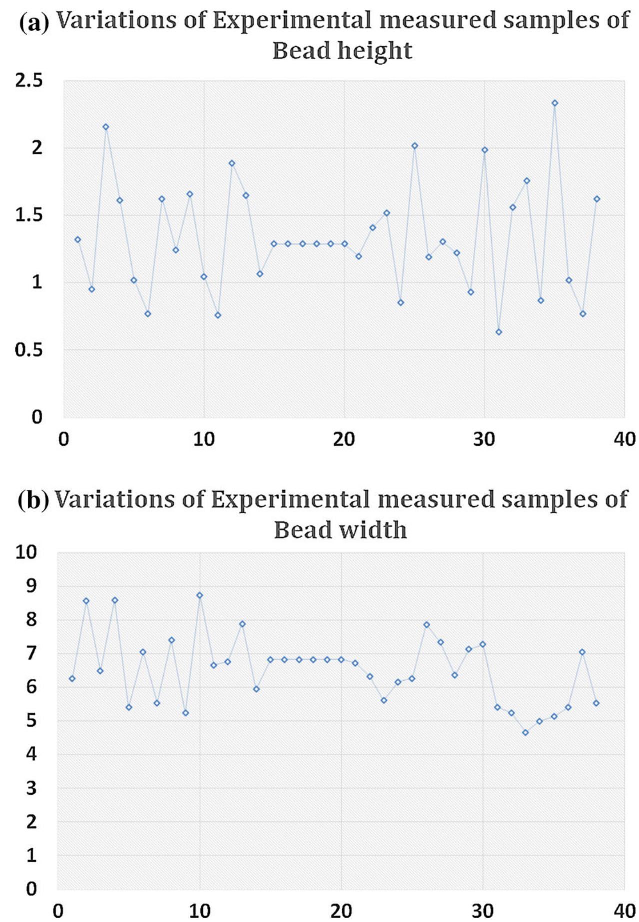

Fig. 2 *Line graph* showing the nature of **a** Bead height (BH). **b** Bead width (BW) with respect to three inputs

quency and the bead geometry size are kept the same as those obtained in (Geng et al. 2015).

In this way, by varying the input conditions (peak current (A), travel speed (m/min) and wire feed speed (m/min)), the bead dimensions (BH and BW) are measured (Table 1). Total of 38 samples are collected from the study measuring bead dimensions based on the varying the three inputs as given in Geng et al. (2015). Figures 2 and 3 show the nature of two bead dimensions (BH & BW) of the WAAM fabricated prototype with respect to the three inputs. Figures 3 and 4 shows that there is high interaction and non-linear correlation between the three inputs and the bead height and bead width. Five-fold Cross-validation (80% training and remaining testing data) approach is deployed to select the appropriate training data set from the five training and five testing data sets based on the minimum mean absolute percentage error (MAPE).

$$Mean\ absolute\ percentage\ error\ (MAPE)\ (\%) = \frac{1}{n}\sum_{i}\left|\frac{A_i - M_i}{A_i}\right| \times 100 \quad (1)$$

where M_i is the predicted value by a model, and A_i is the actual value of the output

Variants of evolutionary algorithms

Multi-gene genetic programming

The present work deploys the genetic programming (Koza 1994) variants for establishing the relationship between the process parameters. One of the popular variant is multi-gene genetic programming (MGGP), which works on mechanism of evolution of the models from the set of genes. The modeling and optimization of the complex manufacturing processes (Liang et al. 2015) has been studied using MGGP. The mechanism (Fig. 4) of the algorithm is as follows:

Step 1 The terminal and function set comprising of three inputs of the process and airthematic functions respectively are set by the user. The set of genes evolved from these sets are combined to form the models.

Step 2 The models performance is computed by fitting the output values obtained from it on the objective function structural risk minimization (SRM) given by

Fig. 3 Scatter matrix showing the correlation between the three inputs and **a** Bead height (BH). **b** Bead width (BW)

$$SRM = \frac{SSE}{n}\left(1 - \left(\sqrt{\left(\frac{j}{n} - \frac{j}{n}\,Log\left(\frac{j}{n}\right) + \frac{Log\left(\frac{j}{n}\right)}{2n}\right)}\right)\right)^{-1} \tag{2}$$

where j equals to order of the polynomial, SSE is the sum of square of error, n is the size of the training set, M_i is the value predicted by a model and Y_i is the actual value of the output. The complexity (j) is defined by the order of the polynomial varying from 1 to 6. The order of the polynomial that best fits the data is the complexity of the model.

Step 3 The models are ranked as per the objective values. If any of the model does not satisfy the termination criterion, the new set of models (new population) is generated using the standard genetic operators such as the crossover, reproduction and mutation.

Step 4 The procedure of producing the new generations continuous unless the termination criterion is not met. In this work, the termination criterion is the number of runs. Each run corresponds to the number of generations, which is also defined by the user.

The parameter setting is adjusted using a trial-and-error approach. The simulations for MGGP are performed in MATLAB R2010 with the parameters such as population size, number of generations, depth of the tree, tournament size, number of iterations set at 400, 120, 8, 6 and 10 respectively. The MGGP method when applied on the WAAM processed data, the Eqs. (4–5) are generated as shown in "Appendix".

Gene expression programming (GEP)

An advanced variant of GP known as gene expression programming (GEP) was developed by Candida Ferreira (2001). GEP is another powerful variant of GP, with only difference between them is that in GEP, the solutions are represented in linear structure or Expression trees (ET) (Fig. 5). This way of defining the tree structures of GP simplifies the diversity of the population.

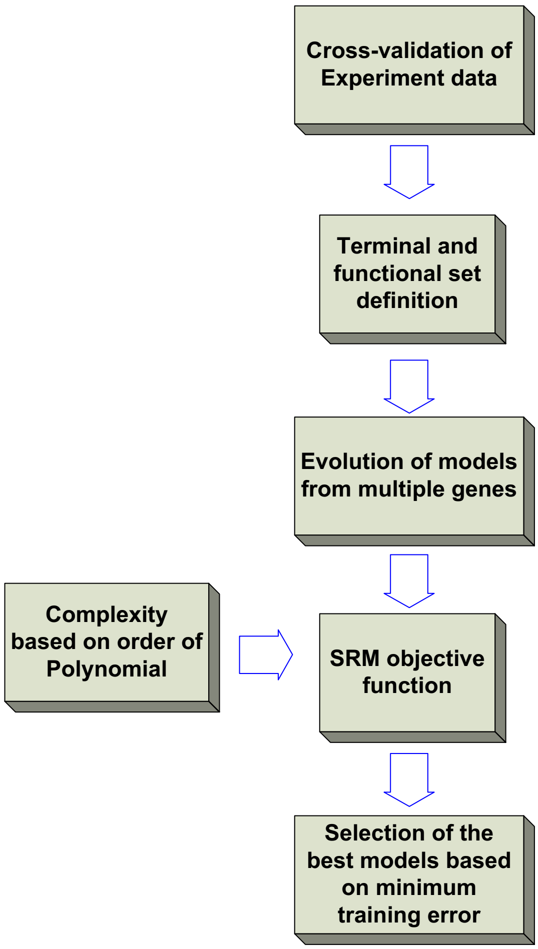

Fig. 4 Mechanism of MGGP algorithm

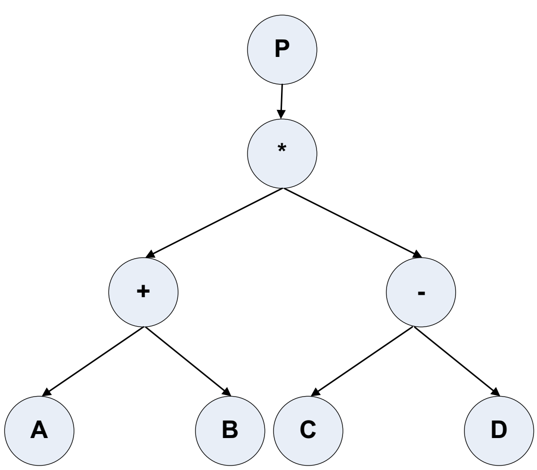

Fig. 5 Mathematical expression represented by *tree*

The linear representation of the ETs is given by

$$\begin{array}{cccccccc} 0 & 1 & 2 & 3 & 4 & 5 & 6 & 7 \\ P & * & + & - & A & B & C & D \end{array} \quad (3)$$

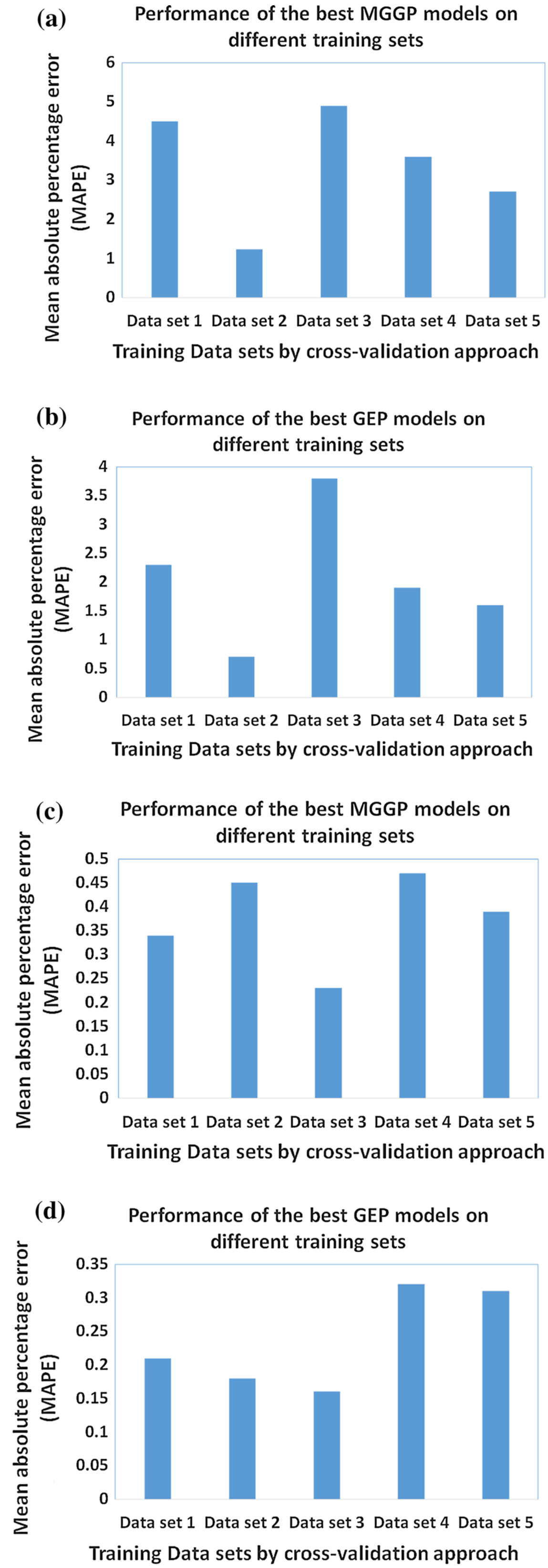

Fig. 6 *Br graph* showing **a** and **b** minimum MAPE for MGGP and GEP models on bead height data set 2 **c** and **d** minimum MAPE for MGGP and GEP models on bead width data set 3

Table 2 Statistical metrics of the bead dimension models

Models	R^2		RMSE (%)		MAPE (%)	
	Training phase	Testing phase	Training phase	Testing phase	Training phase	Testing phase
Bead height (mm)						
MGGP	0.97	0.92	0.029	0.06	1.23	10.92
GEP	0.98	0.99	0.013	0.03	0.70	2.62
Bead width (mm)						
MGGP	0.96	0.93	0.030	0.102	0.23	0.73
GEP	0.99	0.98	0.014	0.020	0.16	0.30

Table 3 Actual and model values obtained from the bead dimension models

No.	Actual BH (mm)	MGGP BH (mm)	GEP BH (mm)	Actual BW (mm)	MGGP BW (mm)	GEP BW (mm)
1	0.928849	0.904845	0.908451	7.127267	7.119676	7.138363
2	1.985034	1.987653	1.959247	7.279766	7.28416	7.245672
3	0.635216	0.637449	0.63531	5.418944	5.441217	5.456515
4	1.562305	1.539545	1.565381	5.245077	5.230549	5.220528
5	1.75587	0.992976	1.699543	4.660088	4.704544	4.680927
6	0.86687	0.927042	0.895195	4.998289	5.049107	5.040942
7	2.334786	2.050188	2.277063	5.131481	5.113188	5.133766
8	1.021051	1.012766	1.038228	5.401869	5.375534	5.385919
9	0.772196	0.761816	0.738456	7.050346	7.104516	7.058387
10	1.623134	1.609771	1.635782	5.53632	5.583049	5.531658

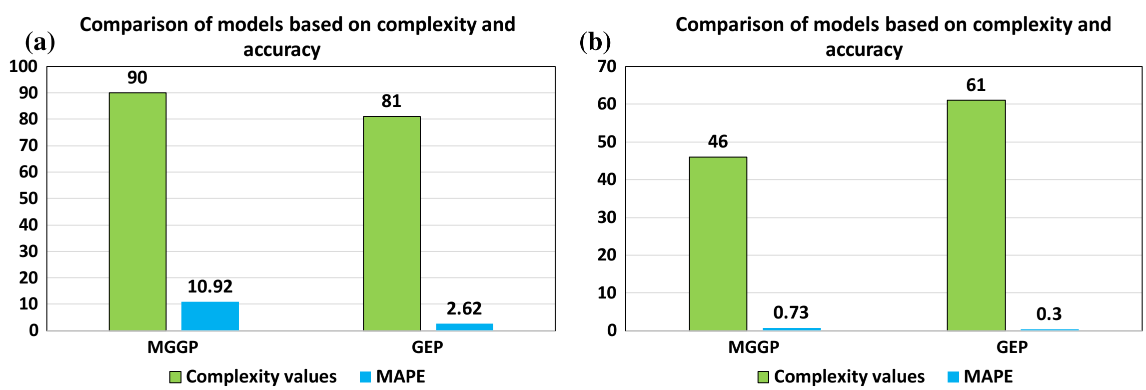

Fig. 7 Complexity and MAPE of the proposed models **a** BH, **b** BW

The past studies (Sabar et al. 2015; Wang et al. 2015a, b) have shown the ability of GEP in modelling the complex processes. The settings in this work for GEP includes the population size of 400, number of generations 100, the maximum depth of the ET as 7 and the number of runs chosen as 20. In the present work, GeneXpro Tool (GEPSOFT 2014) is used to implement GEP on data discussed in "Experimental set-up of WAAM" section in formulating the bead dimensions models (Eqs. 5 and 7 in the "Appendix"). Bar graph shown in Fig. 6 reveals that the mean absolute percentage error (MAPE) of both the models is minimum corresponding to data set 2 for BH and data set 3 for BW models. The best MGGP and GEP models (Eqs. 6 and 7 in the "Appendix") corresponding to data set 2 and data set 3 is therefore selected for analysis of BH and BW respectively. The details numerical investigation of the two models is discussed in "Performance analysis for the bead dimension models".

Performance analysis for the bead dimension models

The performance analysis of the MGGP and GEP models (Eqs. 4–7 in the "Appendix") is conducted by using the metrics (Eqs. 8–10 in "Appendix").

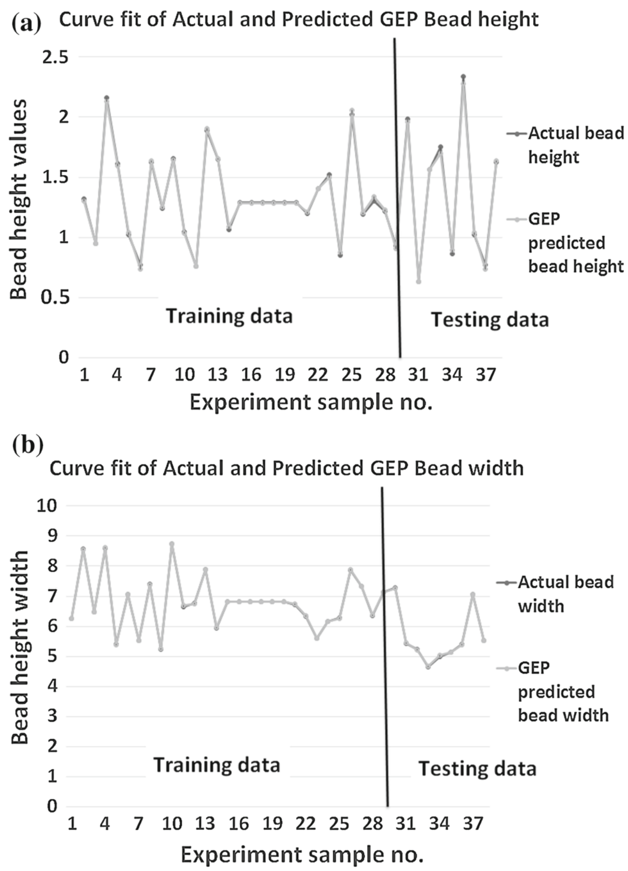

Fig. 8 Fitting plots of the proposed GEP models **a** Bead height, **b** Bead width on training and testing data

Table 2 shows the values of R^2, RMSE and MAPE of the two models for prediction of bead width and bead height. In light of the training aspects, the performance of both the models are comparable. It is clear that the models formulated by GEP have performed better than the MGGP models with R^2achieved as high as 0.99. Table 3 shows the actual and

Table 4 Goodness of fitness tests of the bead dimension models

95% CI	p-values			
	BH		BW	
	MGGP	GEP	MGGP	GEP
Mean paired t-test	0.23	0.36	0.12	0.29
Variance F-test	0.39	0.59	0.26	0.67

predicted values of bead dimensions from the GEP models. Goodness of fit (hypothesis) tests (t-test for mean and f-test for variance) is applied on both the models. It was found that the p-values for all the models for is greater than 0.05, which suggests that the predicted and actual values are close to each other. Figure 7 shows the performance comparison of the two models based on size. It is clear that the GEP models have achieved higher accuracy and lower size of the models. Figure 8a (BH) and Fig. 8b (BW) shows the accurate line curve fitting of the GEP models with respect to the training and testing data. Figure 9a, b illustrates the box plots of the relative error for the GEP models. It shows that the variations, mean, median, maximum and minimum of relative error is quite low (Table 4).

Thus, the analysis depicts that the GEP models for BH and BW have performed better than that of MGGP models.

2D and 3D plots for main and interaction effect of the GEP based bead dimensions models

The 2D and 3D analysis for the GEP models is carried by following the mathematical procedure given in Vijayaraghavan et al. (2015). 2D plots shown in Fig. 10a shows the effect of each input on BH and BW of the process. It clearly shows that the BH decreases non-linearly with an increase in peak current and wire feed speed while increases with an increase

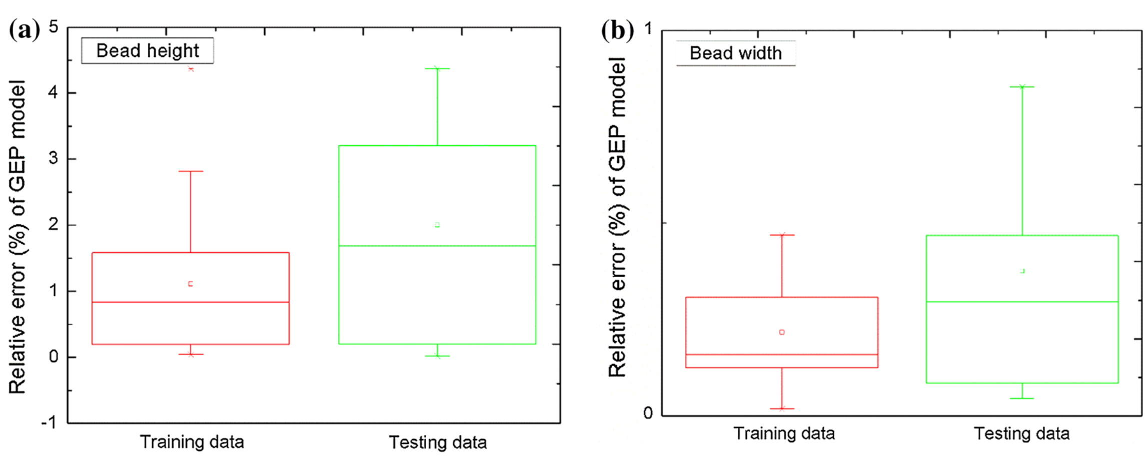

Fig. 9 Statistical distribution of relative error of the GEP model of training and testing data set **a** BH, **b** BW

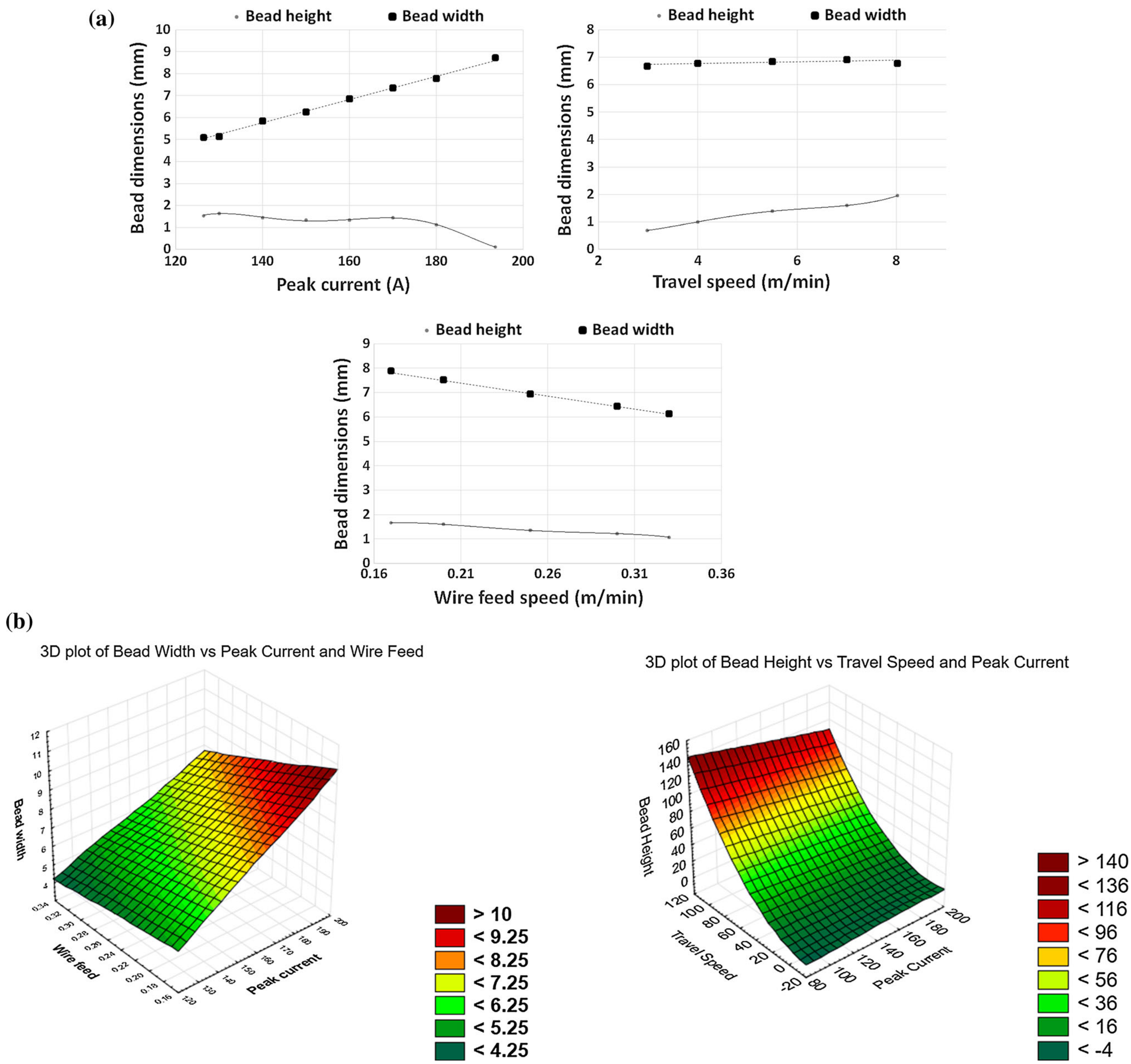

Fig. 10 **a** 2D and **b** 3D plots showing the relationships of the bead height and bead width with respect to the three inputs

in values of travel speed. The decrease rate is higher when the peak current is varied as compared to wire feed speed. On the other hand, the BW increases non-linearly with an increase in values of peak current while decreases with an increase in values of wire feed speed. There was hardly any effect noticed on the impact of travel speed on the BW. The interaction effect between the two inputs on the bead dimensions is evaluated and shown by 3D plots in Fig. 10b. Figure 10b shows that the combined effect of peak current and travel speed on bead height and the combined effect of peak current and wire feed speed on the BW. This indicates that there were higher variations and interaction effect was noticed on the BH than that of the combined effect of inputs on the BW.

Sensitivity of the inputs (Fig. 11) to the bead dimensions is determined by finding range from the 2D plots. It clearly shows that the peak current has the highest influence on the BH values followed by travel speed and wire feed speed. For BW, the peak current also have the highest impact followed by wire feed speed and travel speed. Thus, it can be concluded that the most common and dominant input is peak current which influences both the BH and BW simultaneously. This interpretation from the sensitivity analysis is also in line with the findings from the experimental findings

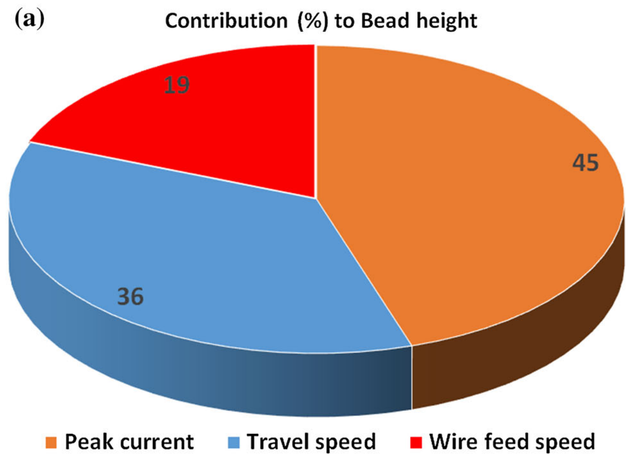

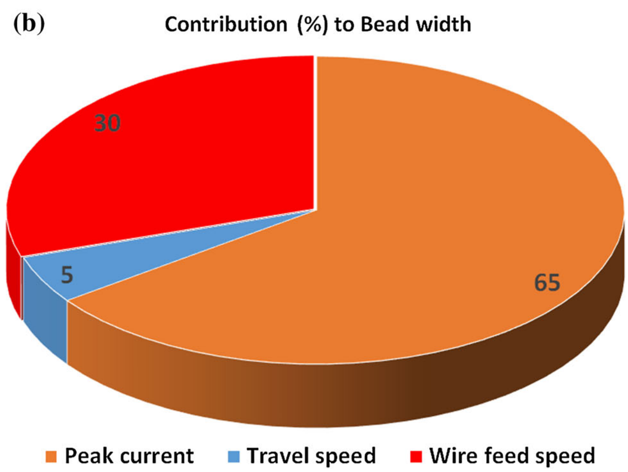

Fig. 11 Percentage contribution of the three inputs to **a** Bead height, **b** Bead width

discussed in Geng et al. (2015). Thus, the statistical performance and the 2D and 3D analysis of the GEP models can be useful in accurate prediction and monitoring of the WAAM process.

Uncertainty analysis of the GEP models for bead height and bead width

The GEP models for bead height and bead width could be simulated in uncertain inputs conditions. The simulation profiler is designed by assuming the inputs as the normal distribution with the minimum and maximum values set same as those of the respective inputs. The analysis could provide us the reliability or the robustness of the models with respect to the variations in inputs. Figure 12a, b shows the distributions resulting from the designed simulation of 5000 iterations. Comparison of both the distributions shows that an approximate normal trend is observed in both the plots of Fig. 12. Figure 12a shows that the distribution is a little skewed towards the right, which suggests that the GEP based bead height model (Fig. 12a) is sensitive to the variations in inputs when compared to the bead width model (Fig. 12b). The reason attributed for this performance could be the non-linear nature of data resulting in such distributions.

Conclusion

This work presents the experimental and evolutionary algorithm variants for study of bead dimensions of the wire and arc additive manufacturing process. The variants of the advanced evolutionary algorithms such as GEP and MGGP are proposed in developing the framework for obtaining the functional expressions for bead height and bead width in circumstance of partial information about the process. These variants provide an alternative to the Response surface methodology, which relies on the statistical assumptions and may induce uncertainty in model formulation. The models developed represents the explicit functions which can be used offline by industry experts for generalization of bead height and bead width values based on the three inputs. This could perhaps avoid the usage of vital experimental resources thus saves time, cost and increases productivity of WAAM process. The performance analysis concluded that the GEP modes for both the bead height and bead width performs better than that of the MGGP models. The uncertainty analysis of the GEP models suggests that the models are reliable and can be used in uncertain input conditions. The findings from 2D and 3D analysis reported that the peak current and travel speed influences the bead height the most whereas the peak current and wire feed speed influences the bead width the most. The most dominant input influencing the bead height and bead width was found to be peak current. Future work for authors is to upgrade the WAAM process by addition of inputs such as the machine type and arc type generation and then experimentally and numerically investigate the process and evaluate any physically differences based on the current study.

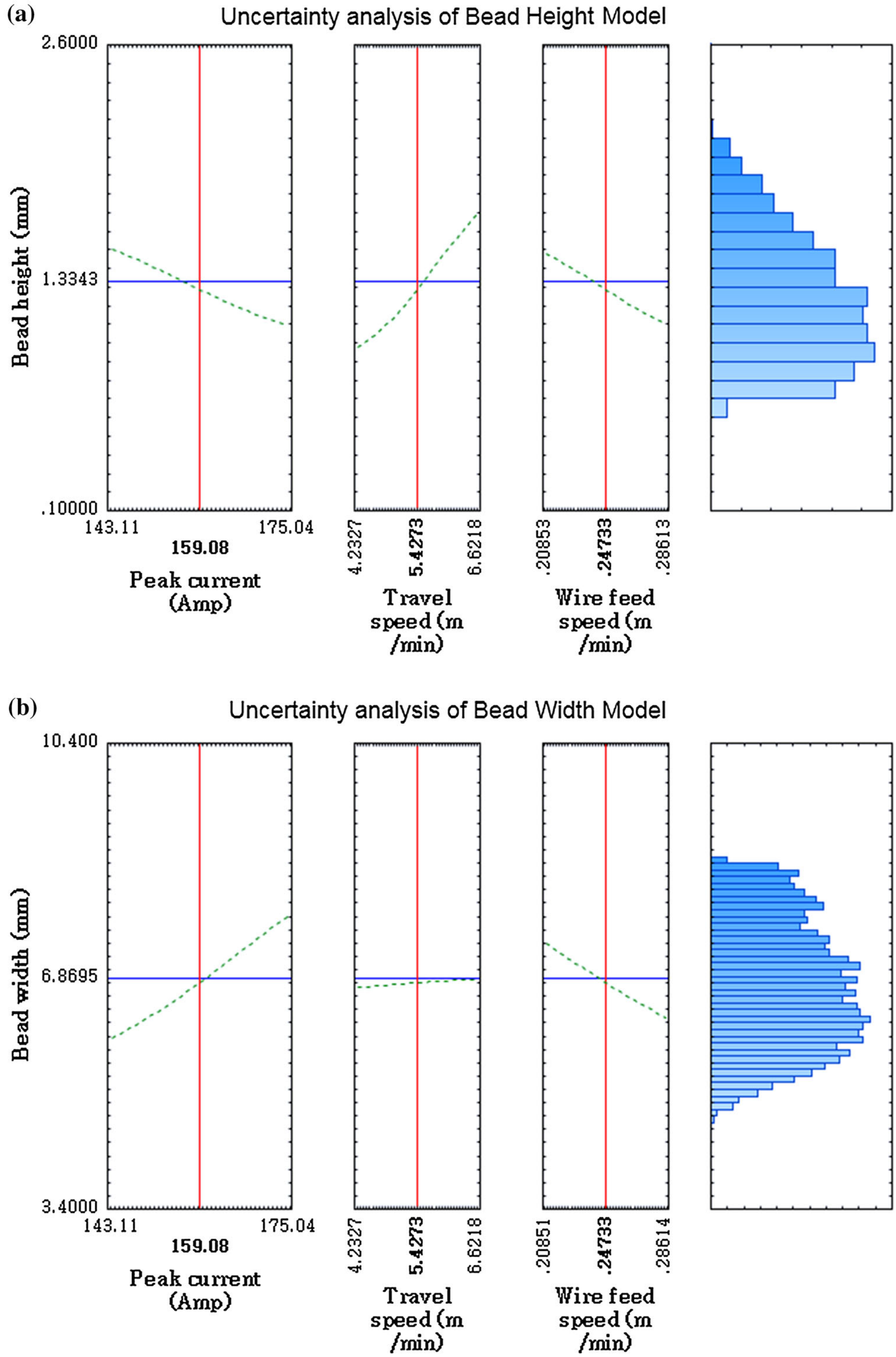

Fig. 12 Simulation profiler for GEP models with variations in the inputs from its mean values **a** Bead height model, **b** Bead width model

Acknowledgements This study was supported by Shantou University Scientific Research Funded Project (Grant No. NTF 16002)

Appendix

$$\begin{aligned}
&\text{Bead height}_{\text{MGGP}}(mm) = -0.11195 + (-8.8995e - 006)^{*}\\
&\quad((\tan(((x2) - ((\tan(x1))^{*}(\exp(x3))))^{*}(x1)))\\
&\quad - (\cos(\sin(x1)))) + (0.015439)^{*}(\tan((x2) - ((\tan(x1))^{*}\\
&\quad(\exp(x3))))) + (0.054744)^{*}(\tan((\exp(\tan(x1))))^{*}\\
&\quad((\tan(\tanh(x1)))^{*}((\exp(x3))^{*}(\tanh(\tan(x1)))))))\\
&\quad + (0.70311)^{*}((x2) - ((x2)^{*}(x3))) + (0.0036055)^{*}(((x1)\\
&\quad - ((x1)^{*}((1.158172)))) - ((\tan((x2)\\
&\quad -((x2)^{*}(x3))))^{*}(\tan(x1)))) + (-0.0052258)\\
&\quad ^{*}((\tan((x1)^{*}(x3)))^{*}(\cos((\tan(((x2)\\
&\quad -(x2))^{*}(x1))) - ((x1)^{*}(\tan((x1)^{*}(x3)))))))\\
&\quad +(0.0018798)^{*}((x1) - ((x1)^{*}(x2)))\\
&\quad + (-0.022407)^{*}(\tan((\exp(\tanh(x2)))^{*}((\tan(x3))^{*}(x2)))) \qquad (4)
\end{aligned}$$

$$\begin{aligned}
&\text{Bead height}_{\text{GEP}}(mm) = -0.27529 + (0.0029583)^{*}\\
&\quad(\tan((\tan((x2)^{*}((14.502281))))^{*}(x1))) + (-0.029465)^{*}\\
&\quad(\cos(((\tanh(x2)) + ((x2)^{*}(\tan((x3)^{*}(x1)))))^{*}(x1)))\\
&\quad + (-0.20681)^{*}(((\tan((x3)^{*}(x1)))^{*}(x3))^{*}(x3))\\
&\quad + (-0.0015171)^{*}((x2)^{*}(x1)) + (-0.6226)^{*}((\tanh(\cos((x3)\\
&\quad + ((3.678354))))) + ((x2)^{*}((\tanh(x3))\\
&\quad - (\tanh((14.502281)))))) + (-0.019202)^{*}\\
&\quad((\sin(\sin((plog(x1))^{*}((x2)^{*}(\exp(x2))))))\\
&\quad + (\sin(\sin((plog(x1))^{*}((x1)^{*}(\exp(x2)))))))\\
&\quad + (0.041126)^{*}((\tan((x2)^{*}(x1)))^{*}(x3)) + (0.0012584)^{*}\\
&\quad((\tan((\tanh(x3))^{*}(x1)))^{*}((x2)^{*}((\tanh(x3))\\
&\quad - (\tanh((14.502281)))))) \qquad (5)
\end{aligned}$$

$$\begin{aligned}
&\text{Bead width}_{\text{MGGP}}(mm) = 4.5428 + (0.08313)^{*}((x1) - (x2))\\
&\quad + (-0.0093962)^{*}((\exp(\tan(x1))) + ((x1) - (x2)))\\
&\quad + (-0.19108)^{*}((\sin(((-15.924689)) - (x3)))^{*}(((x3)^{*}(x1))\\
&\quad - (x2))) + (34.0543)^{*}(plog(\sin(((-15.924689)) - (x3))))\\
&\quad + (-14.6929)^{*}(plog(x3)) + (0.032877)^{*}(\sin((((\sin(x3))^{*}\\
&\quad(x1)) - (x2)) - (x2))) + (0.093567)^{*}(\exp(\cos(x2)))\\
&\quad + (0.74232)^{*}(\cos(\sin(\cos((\exp(x1)) + (x2))))) \qquad (6)
\end{aligned}$$

$$\begin{aligned}
&\text{Bead width}_{\text{GEP}}(mm) = -4.2408 + (-0.00047266)^{*}\\
&\quad((x1)^{*}(((x1) - (x2))^{*}(x3)))\\
&\quad +(-0.18222)^{*}(\cos(\tan(\exp(x1))))\\
&\quad + (-0.06944)^{*}(\cos(\tan(((x1) - (x2))^{*}(x3))))\\
&\quad + (0.089221)^{*}(x1) + (-0.12007)^{*}(\cos(\cos(\tan(((x1)\\
&\quad - (x2))^{*}(x3))))) + (-0.054305)^{*}\\
&\quad(\sin(\sin(\sin(\tan(plog(\tan(x3)))))))\\
&\quad + (-0.030142)^{*}(\sin(((((x1) - (x2))^{*}(x3))\\
&\quad + (plog(\tan(((-4.416740))^{*}(x2)))))\\
&\quad +(\sin(\tan(plog(\sin(x2))))))\\
&\quad + (0.075278)^{*}(\sin((plog(\tan(x3))) + (\tan(\tan(\tan(x2)))))) \qquad (7)
\end{aligned}$$

$$Coefficient\ of\ \det er\ \min ation\ (R^2) = \left(\frac{\sum_{i=1}^{n}(A_i - \overline{A_i})(M_i - \overline{M_i})}{\sqrt{\sum_{i=1}^{n}(A_i - \overline{A_i})^2 \sum_{i=1}^{n}(M_i - \overline{M_i})^2}}\right)^2 \qquad (8)$$

$$Root\ mean\ square\ error\ (RMSE) = \sqrt{\frac{\sum_{i=1}^{N}|M_i - A_i|^2}{N}} \qquad (9)$$

$$Relative\ error\ (\%) = \frac{|M_i - A_i|}{A_i} \times 100 \qquad (10)$$

References

Baufeld, B., Brandl, E., & van der Biest, O. (2011). Wire based additive layer manufacturing: Comparison of microstructure and mechanical properties of Ti6Al4V components fabricated by laser-beam deposition and shaped metal deposition. *The Journal of Materials Processing Technology*, *211*(6), 1146–1158.

Brandl, E., Achim, S., & Christoph, L. (2012). Morphology, microstructure, and hardness of titanium (Ti-6Al-4V) blocks deposited by wire-feed additive layer manufacturing (ALM). *Materials Science and Engineering: A*, *532*, 295–307.

Çiçek, A., Kıvak, T., & Ekici, E. (2015). Optimization of drilling parameters using Taguchi technique and response surface methodology (RSM) in drilling of AISI 304 steel with cryogenically treated HSS drills. *Journal of Intelligent Manufacturing*, *26*(2), 295–305.

Ding, D., et al. (2016). Automatic multi-direction slicing algorithms for wire based additive manufacturing. *Robotics and Computer-Integrated Manufacturing*, *37*, 139–150.

Ding, D., Pan, Z., Cuiuri, D., & Li, H. (2015). A multi-bead overlapping model for robotic wire and arc additive manufacturing (WAAM). *Robotics and Computer-Integrated Manufacturing*, *31*, 101–110.

Ferreira C. (2001). *Gene expression programming: A new adaptive algorithm for solving problems*. arXiv preprint arXiv:cs/0102027.

Garg, A., & Tai, K. (2012). Comparison of Regression Analysis, Artificial Neural Network and Genetic Programming in Handling the Multicollinearity Problem, In *Proceedings of International Conference on Modelling, Identification & Control (ICMIC2012)*, Wuhan, China, 24–26 (pp.353-358).

Garg, A., et al. (2014). A molecular simulation based computational intelligence study of a nano-machining process with implications on its environmental performance. *Swarm and Evolutionary Computation*, *21*, 54–63.

Garg, A., Lam, Jasmine Siu Lee, & Savalani, M.M. (2015) Laser power based surface characteristics models for 3-D printing process. *Journal of Intelligent Manufacturing*, pp. 1–12. doi:10.1007/s10845-015-1167-9

Geng, Haibin, et al. (2015). A prediction model of layer geometrical size in wire and arc additive manufacture using response surface methodology. *The International Journal of Advanced Manufacturing Technology,* pp. 1–12. doi:10.1007/s00170-015-8147-2

GEPSOFT, GeneXproTools, Version 5.0, http://www.gepsoft.com (2014).

Gibson, Ian, Rosen, David W., & Stucker, Brent. (2010). *Additive manufacturing technologies* (Vol. 238). New York: Springer.

Kazanas, P., Deherkar, P., Almeida, P., et al. (2012). Fabrication of geometrical features using wire and arc additive manufacture. *Journal of Engineering Manufacture*, *226*(6), 1042–1051.

Koza, J. R. (1994). *Genetic programming II: Automatic discovery of reusable programs*. Cambridge, USA: MIT.

Liang, C., Li, M., Lu, B., Gu, T., Jo, J., & Ding, Y. (2015). Dynamic configuration of QC allocating problem based on multi-objective genetic algorithm. *Journal of Intelligent Manufacturing*, 1–9, doi:10.1007/s10845-015-1035-7.

Mahapatra, S. S., & Panda, B. N. (2013). Benchmarking of rapid prototyping systems using grey relational analysis. *International Journal of Services and Operations Management*, *16*(4), 460–477.

Nie, L., Gao, L., Li, P., & Li, X. (2013). A GEP-based reactive scheduling policies constructing approach for dynamic flexible job shop scheduling problem with job release dates. *Journal of Intelligent Manufacturing*, *24*(4), 763–774.

Oshima, K., Xiang, X., & Yamane, S. (2005). Effects of power source characteristic on CO_2 short circuiting arc welding. *Science and Technology of Welding and Joining*, *10*(3), 281–286.

Ouyang, J. H., Wang, H., & Kovacevic, R. (2002). Rapid prototyping of 5356-aluminum alloy based on variable polarity gas tungsten arc welding: process control and microstructure. *Materials and Manufacturing Processes*, *17*(1), 103–124.

Panda, B. N., Bahubalendruni, M. V. A. Raju, & Biswal, B. B. (2014). A general regression neural network approach for the evaluation of compressive strength of FDM prototypes. *Neural Computing and Applications*, *26*(5), 1–8.

Panda, B., Garg, A., Jian, Z., Heidarzadeh, A., & Gao, L. (2016a). Characterization of the tensile properties of friction stir welded aluminum alloy joints based on axial force, traverse speed, and rotational speed. *Frontiers of Mechanical Engineering*, *11*(3), 289–298.

Panda, B.N., Bahubalendruni, R.M., Biswal, B.B., & Leite, M., (2016b) A CAD-based approach for measuring volumetric error in layered manufacturing. Proceedings of the Institution of Mechanical Engineers, *Part C: Journal of Mechanical Engineering Science*, doi:10.1177/0954406216634746.

Panda, B.N., Shankhwar, K., Garg, A., & Jian, Z. (2016c). Performance evaluation of warping characteristic of fused deposition modelling process. *The International Journal of Advanced Manufacturing Technology.* doi:10.1007/s00170-016-8914-8.

Rao, K. V., & Murthy, P. B. G. S. N. (2016). Modeling and optimization of tool vibration and surface roughness in boring of steel using RSM, ANN and SVM. *Journal of Intelligent Manufacturing*, 1–11, doi:10.1007/s10845-016-1197-y.

Sabar, N. R., Ayob, M., Kendall, G., & Qu, R. (2015). Automatic design of a hyper-heuristic framework with gene expression programming for combinatorial optimization problems. *IEEE Transactions on Evolutionary Computation*, *19*(3), 309–325.

Sharma, N., Kumar, K., Raj, T., & Kumar, V. (2016) Porosity exploration of SMA by Taguchi, regression analysis and genetic programming. *Journal of Intelligent Manufacturing.* doi:10.1007/s10845-016-1236-8.

Sohrabpoor, H., et al. (2016). Analysis of laser powder deposition parameters: ANFIS modeling and ICA optimization. *Optik-International Journal for Light and Electron Optics*, *127*(8), 4031–4038.

Tay, Y. W., et al. (2016). Processing and properties of construction materials for 3D printing. *Materials Science Forum*, *861*, 177–181.

Vijayaraghavan, V. et al (2014) Density characteristics of laser-sintered three-dimensional printing parts investigated by using an integrated finite element analysis–based evolutionary algorithm approach. *Proceedings of the Institution of Mechanical Engineers, Part B: Journal of Engineering Manufacture (Imeche)*, doi:10.1177/0954405414558131

Vijayaraghavan, V., Garg, A., Lam, J. S. L., Panda, B., & Mahapatra, S. S. (2015). Process characterization of 3D-printed FDM components using improved evolutionary computational approach. *The International Journal of Advanced Manufacturing Technology*, *78*(5–8), 781–793.

Wang, F., Williams, S., & Rush, M. (2011). Morphology investigation on direct current pulsed gas tungsten arc welded additive layer manufactured Ti6Al4V alloy. *The International Journal of Advanced Manufacturing Technology*, *57*(5–8), 597–603.

Wang, L., Yang, B., Wang, S., & Liang, Z. (2015a). Building image feature kinetics for cement hydration using gene expression programming with similarity weight tournament selection. *IEEE Transactions on Evolutionary Computation*, *19*(5), 679–693.

Wang, P., Emmerich, M., Li, R., Tang, K., Back, T., & Yao, X. (2015b). Convex hull-based multiobjective genetic programming for maximizing receiver operating characteristic performance. *IEEE Transactions on Evolutionary Computation*, *19*(2), 188–200.